ELSEVIER

www.elsevier.nl/locate/ica

Inorganica Chimica Acta 305 (2000) 19–25

Inorganica Chimica Acta

# Structure and single crystal EPR study of Cu(II)(L-threonine)$_2$·H$_2$O

Alberto C. Rizzi [a], Oscar E. Piro [b], Eduardo E. Castellano [c], Otaciro R. Nascimento [c], Carlos D. Brondino [a,*]

[a] *Departamento de Física, Facultad de Bioquímica y Ciencias Biológicas, Universidad Nacional del Litoral, CC 242, 3000 Santa Fe, Argentina*
[b] *Departamento de Física, Facultad de Ciencias Exactas, Universidad Nacional de La Plata and Programa PROFIMO (CONICET), CC 67, 1900 La Plata, Argentina*
[c] *Instituto de Física de São Carlos, Universidade de São Paulo, CP 369, 13560 São Carlos SP, Brazil*

Received 10 November 1999; accepted 28 February 2000

**Abstract**

We report the structure and single crystal EPR studies at 9.8 and 33.3 GHz of the title compound, [Cu(C$_4$H$_8$NO$_3$)$_2$]·H$_2$O. The Cu(II) ion is in an elongated octahedral environment equatorially *trans*-coordinated by two oxygen atoms and two nitrogen atoms of threonine molecules which act as bidentate ligands (mean $d$(Cu–O) = 1.95(1) and $d$(Cu–N) = 1.98(1) Å). It is axially coordinated by carboxylic oxygen atoms belonging to a pair of molecules translated in $\pm b$ (Cu–O distances of 2.478(8) and 2.972(3) Å). This axial O···Cu···O interaction gives rise to infinite copper ion chains along the $b$ crystal axis. Neighboring chains are coupled through complex chemical paths including H-bonds and the amino acid side chain. Single crystal EPR spectra show a single, exchange-collapsed resonance at both microwave frequencies for any magnetic field orientation. We evaluated the crystal and the molecular $\boldsymbol{g}$-tensors from the angular variation of the EPR line position. The results ($g_\perp = 2.060(2)$ and $g_\parallel = 2.240(3)$) indicate that the electronic ground orbital of the Cu ions is mainly of the $3d_{x^2-y^2}$ type. The analysis of the angular variation of the EPR linewidth allows us to estimate a mean exchange coupling constant $|J/k| = 1.45(5)$ K for the inter-chain chemical paths.


*Keywords:* Crystal structures; Super-exchange; Copper complexes; Amino acid complexes

## 1. Introduction

The study of exchange-coupled molecular systems has been a multidisciplinary field of continuous interest during the past few years. Major efforts have been directed to the study of systems where the magnetic interactions are transmitted through short chemical paths [1]. These studies made it possible to design molecular systems with predictable magnetic properties [2]. However, there are not many studies of magnetic interactions transmitted through long distances. Both theoretical and experimental work is clearly necessary to clarify this problem. In addition, it may also be relevant to understand biological systems, which show magnetically coupled redox centers connected by long chemical paths, which are supposed to be involved in electronic transfer processes [3].

Copper–amino acid complexes are appropriated systems to study these problems. In these systems, electronic paths, such as H-bonds, carboxylate bridges, saturated and non-saturated hydrocarbon chains, and stacking of aromatic rings connect the metal ions and are involved in the transmission of weak super-exchange interactions between the paramagnetic centers [4–7]. The exchange coupling constants ($J$) associated with these paths are in the range $0.0005 \leq |J/k| \leq 2$ K, and therefore, are difficult to evaluate by standard magnetic susceptibility measurements. It has been shown, however, that they can be accurately and selectively measured employing EPR, by monitoring the changes in the spectrum due to exchange narrowing, collapse of the hyperfine structure, merging effect, etc. [8,9].

* Corresponding author. Fax: +54-342-457 5221.
*E-mail address:* brondino@fbcb.unl.edu.ar (C.D. Brondino)

0020-1693/00/$ - see front matter 
PII: S0020-1693(00)00105-5

Here we report EPR studies of single crystals of bis(L-threonine) copper(II) monohydrate, Cu(L-threon)$_2$·H$_2$O. This compound shows carboxylate bridged copper ion chains, which are linked through mixed chemical paths involving the amino acid side chain and hydrogen bonds. Amirthalingam and Muralidharan solved the structure of the compound several years ago [10]. The final *R* factor was 10%. In order to analyze the magnitudes of the super-exchange interactions between metal ions, a more accurate crystal structure re-determination was performed and is also reported here.

Table 1
Crystal data and summary of intensity data collection and structure refinement for Cu(L-threon)$_2$·H$_2$O

| | |
|---|---|
| Formula | $C_8H_{18}CuN_2O_7$ |
| Color | deep blue–violet |
| Shape | parallelepiped |
| Formula weight | 317.78 |
| Space group | $P2_1$ |
| Temperature (°C) | 22 |
| Unit cell dimensions [a] | |
| $a$ (Å) | 11.104(3) |
| $b$ (Å) | 4.890(2) |
| $c$ (Å) | 11.210(3) |
| $\beta$ (°) | 94.35(2) |
| $V$ (Å$^3$) | 606.9(3) |
| Formula units per unit cell | 2 |
| $D_{calc}$ (g cm$^{-3}$) | 1.739 |
| $\mu_{calc}$ (cm$^{-1}$) | 18.3 |
| Diffractometer | Enraf–Nonius CAD-4 |
| Scan | $\omega$–2$\theta$ |
| Radiation, graphite monochromator | Mo K$\alpha$ ($\lambda = 0.71069$ Å) |
| Crystal size (mm) | $0.02 \times 0.07 \times 0.22$ |
| Scan width | $0.8 + 0.35 \tan\theta$ |
| Standard reflection | −4 0 2 |
| Decay of standard (%) | ±1.5 |
| Reflections measured | 1707 |
| 2$\theta$ Range (°) | $2 \leq 2\theta \leq 50$ |
| Range of $h$, $k$, $l$ | ±13, −1 to 5, −1 to 13 |
| No. observed reflections [$F_o \geq 6\sigma(F_o)$] [b] | 1031 |
| Computer programs [c] | SHELX, SDP |
| Structure solution [d] | SHELX |
| No. parameters varied | 163 |
| Minimized function | $\Sigma w(\|F_o\| - \|F_c\|)^2$ |
| Weights, $w$ | $[\sigma(F_o)^2 + 0.003F_o^2]^{-1}$ |
| GOF | 0.9 |
| $R = \Sigma\|\|F_o\| - \|F_c\|\|/\Sigma\|F_o\|$ | 0.045 |
| $R_w = [\Sigma w(\|F_o\| - \|F_c\|)^2/\Sigma w\|F_o\|^2]^{0.5}$ | 0.046 |
| Largest difference peak and hole (e Å$^{-3}$) | 0.68 and −0.88 |

[a] Least-squares refinement of $[(\sin\theta)/\lambda]^2$ values for 21 reflections in the range $15.8 < 2\theta < 36.0°$.

[b] Corrections: Lorentz, polarization and absorption.

[c] Neutral scattering factors and anomalous dispersion corrections.

[d] Structure solved by Patterson and Fourier methods and the final molecular model obtained by anisotropic full-matrix least-squares refinement for the non-H atoms. The hydrogen atoms of the oxydryl groups, of one amino terminal and of one alpha carbon were located in a difference Fourier map that also showed one of the water hydrogen atoms. The other, non-water, hydrogen atoms were positioned stereochemically. All were included fixed in the molecular model and their common isotropic thermal parameter converged to $U = 0.061$ Å$^2$ in the final refinement. A test of chirality was performed to determine the absolute molecular conformation; upon changing to the other stereoisomer, the *R* factor increased from 0.045 to 0.052.

## 2. Experimental

### 2.1. Sample preparation

All commercially available chemicals were reagent grade and used as received. L-Threonine (2 mmol) was dissolved in 10 ml of ion-exchanged water. The solution, into which 0.5 mmol of basic copper carbonate was added, was stirred for a few minutes until an intense blue color developed, and then filtered using a 0.22 μm Millipore filter. The filtrate was left to evaporate slowly at room temperature (r.t.). After 1 week thin blue single crystals were obtained. They grow as thin plates parallel to the *ab* plane, with a well-defined *b* direction, a fact that simplifies the orientation of the samples.

### 2.2. Diffraction data and structure solution and refinement

Crystal data, data collection procedures, structural determination methods, and refinement results for Cu(L-threon)$_2$·H$_2$O are summarized in Table 1 [11–13].

### 2.3. EPR measurements

The EPR data at 9.8 GHz (X-band) were obtained with a Bruker ER-200 EPR spectrometer, using a 12-inch rotating magnet, and a Bruker cylindrical cavity working in the TE011 mode and 100 kHz field modulation. A Varian E-line spectrometer and a cylindrical cavity were used for the 33.3 GHz (Q-band) measurements. All experiments were carried out at r.t.

Single crystal samples were oriented by gluing the (001) face to a cleaved KCl cubic holder: a set $x$, $y$, $z$ of orthogonal axes was defined, with the $x$ and $y$ directions along the $a$ and $b$ crystal axes, respectively, and the $z$ axis along the $c^* = a \times b$ direction. The sample holder was positioned in a horizontal plane at the top of a pedestal in the center of the microwave cavity, so that the applied magnetic field could be accurately rotated in the *ab*, *c*a* or *c*b* planes of the sample.

## 3. Results and discussion

### 3.1. Structural results

Fig. 1 is an ORTEP drawing of a molecule of the compound showing the coordination around the Cu(II)

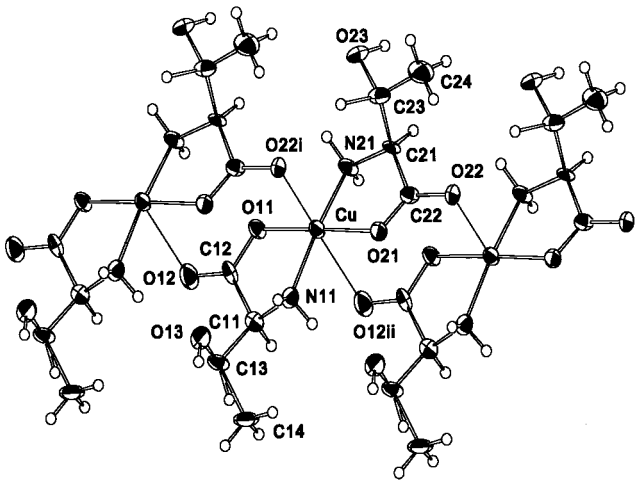


Fig. 1. ORTEP projection along *a* of Cu(L-threon)$_2$·H$_2$O showing the coordination sphere around the Cu(II) ion and part of a polymeric chain along the *b* axis. The water molecule is not included. Symmetry code: (i) $x$, $y-1$, $z$; (ii) $x$, $y+1$, $z$.

ion, the labeling of the non-H atoms, and their displacement ellipsoids [14]. Selected bond distances and angles are in Table 2, including the hydrogen bonding parameters corresponding to the superexchange paths, which will be discussed later. Fractional coordinates and equivalent isotropic temperature parameters [15] for Cu(L-threon)$_2$·H$_2$O are available as supplementary material (see Section 5).

The copper ion is in an elongated octahedral coordination. *Trans* coordination by two threonine molecules produces a practically square planar (within $\pm$0.05(1) Å) equatorial $N_2O_2$ ligand group (mean Cu–$O_{eq}$ and Cu–$N_{eq}$ bond distances are 1.95(1) and 1.98(1) Å, respectively). The Cu(II) ion is 0.079(1) Å out-of-plane, towards the closest axial oxygen ligands ($O_{ax}$). The axial ligands are carboxylate oxygen atoms of a pair of symmetry related molecules obtained through $\pm b$ translations (Cu–$O_{ax}$ distances of 2.478(8) and 2.972(3) Å, respectively). This axial interaction gives place to polymeric infinite –Cu–$O_{eq}$–C–$O_{ax}$–Cu– chains along the *b* axis (see Fig. 1), similar to those found in *trans*-bis(L-2-aminobutyrato) copper(II) [16] (Cu(L-but)$_2$, where the Cu–$O_{ax}$ distances are 2.679(5) and 2.787(5) Å), and in the closely related *trans*-bis(D,L-2-aminobutyrato) copper(II) (Cu(D,L-but)$_2$, where the Cu–$O_{ax}$ distances are 2.758(3) Å and the Cu(II) ion is on a center of symmetry) [17]. The copper ions in a chain are also connected by a hydrogen bond between $N_{eq}$ and the hydroxyl O of the amino acid side chain. As reported for these compounds, it is expected that the

Table 2
Selected interatomic bond distances (Å) and angles (°) for Cu(L-threon)$_2$·H$_2$O, including hydrogen bonds [a,b,c,d]

| | | | |
|---|---|---|---|
| *Bond lengths* | | | |
| Cu–O(11) | 1.941(7) | Cu–N(21) | 1.982(8) |
| Cu–N(11) | 1.968(8) | Cu–O(22$^{i}$) | 2.478(8) |
| Cu–O(21) | 1.957(7) | Cu–O(12$^{ii}$) | 2.972(9) |
| *Bond angles* | | | |
| O(11)–Cu–N(11) | 83.6(3) | N(11)–Cu–O(22$^{i}$) | 93.2(3) |
| O(11)–Cu–O(21) | 177.5(3) | N(11)–Cu–O(12$^{ii}$) | 86.5(3) |
| O(11)–Cu–N(21) | 96.2(3) | O(21)–Cu–O(22$^{i}$) | 92.8(3) |
| N(11)–Cu–O(21) | 96.4(3) | O(21)–Cu–O(12$^{ii}$) | 87.1(3) |
| N(11)–Cu–N(21) | 172.1(3) | N(21)–Cu–O(22$^{i}$) | 94.7(3) |
| O(21)–Cu–N(21) | 83.4(3) | N(21)–Cu–O(12$^{ii}$) | 85.6(3) |
| O(11)–Cu–O(22$^{i}$) | 89.7(3) | O(22$^{i}$)–Cu–O(12$^{ii}$) | 179.6(2) |
| O(11)–Cu–O(12$^{ii}$) | 90.4(3) | | |

*Hydrogen bond distances and angles*

| D | H | A | D···A | H···A [d] | ∠ D–H···A [d] | D–H [d] |
|---|---|---|---|---|---|---|
| O(23) | H(O23) | O(w) | 2.72(1) | 1.66(1) | 173.3(5) | 1.061(8) |
| O(w) | H(Ow) | O(23$^{iii}$) | 2.91(1) | 1.928(7) | 155.9(6) | 1.038(6) |
| O(w) | [c] | O(12$^{iv}$) | 2.90(1) | [c] | [c] | [c] |
| O(13) | H(O13) | O(22$^{v}$) | 2.75(1) | 1.89(1) | 159.7(5) | 0.91(1) |
| N(11) | H(N11) | O(13$^{ii}$) | 2.84(1) | 1.99(1) | 161.4(6) | 0.89(1) |

[a] Symmetry code: (i) $x$, $y-1$, $z$; (ii) $x$, $y+1$, $z$; (iii) $-x$, $y+1/2$, $-z-1$; (iv) $-x$, $y+3/2$, $-z$; (v) $1-x$, $y-3/2$, $-z$.

[b] Donor and acceptor atoms are indicated by D and A, respectively. All hydrogen bond distances with D···A distance up to 3 Å are included.

[c] Presumed H-bonds as the corresponding hydrogen atom of the water molecule could not be located in the final difference Fourier map (see text).

[d] Standard deviations of distances and angles involving hydrogen atoms are only estimative as in the refinement these atoms were kept at a fixed distance from the atom to which they are bonded (see footnote to Table 1).

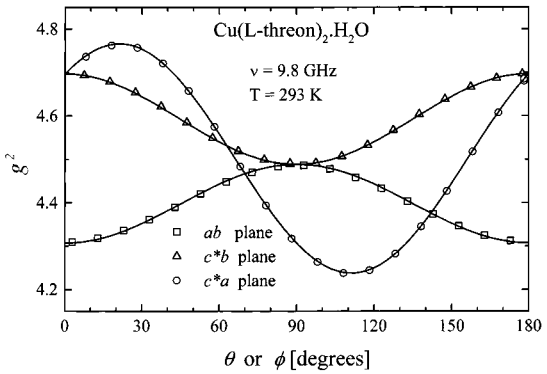


Fig. 2. Angular variation of the squared $g$-factor measured at 298 K and 9.8 GHz in three orthogonal planes of Cu(L-threon)$_2$·H$_2$O single crystal. The solid lines were obtained by fitting the data with a symmetric $\boldsymbol{g}^2$ second-order tensor. The parameters of the fit are included in Table 3.

Table 3
Values of the components of the $\boldsymbol{g}^2$ tensor obtained by least-squares analyses of the data at each microwave frequency [a]

| 9.8 GHz | 33.3 GHz |
|---|---|
| $(g^2)_{xx} = 4.3072(4)$ | $(g^2)_{xx} = 4.2762(7)$ |
| $(g^2)_{yy} = 4.4882(4)$ | $(g^2)_{yy} = 4.4942(7)$ |
| $(g^2)_{zz} = 4.6968(4)$ | $(g^2)_{zz} = 4.7202(7)$ |
| $(g^2)_{zx} = 0.1784(5)$ | $(g^2)_{zx} = 0.1506(8)$ |
| $(g^2)_{xy} = (g^2)_{zy} = 0$ | $(g^2)_{xy} = (g^2)_{zy} = 0$ |
| $(g^2)_1 = 4.2378(5)$ | $(g^2)_1 = 4.2299(8)$ |
| $(g^2)_2 = 4.7661(5)$ | $(g^2)_2 = 4.7664(8)$ |
| $(g^2)_3 = 4.4882(4)$ | $(g^2)_3 = 4.4942(6)$ |
| $\mathbf{a}_1 = [0.9321(3), 0, -0.3623(8)]$ | $\mathbf{a}_1 = [0.9559(4), 0, -0.2940(1)]$ |
| $\mathbf{a}_2 = [0.3623(8), 0, 0.9321(3)]$ | $\mathbf{a}_2 = [0.2940(1), 0, 0.9559(4)]$ |
| $\mathbf{a}_3 = [0, 1, 0]$ | $\mathbf{a}_3 = [0, 1, 0]$ |
| $g_\perp = 2.060(2)$ | $g_\perp = 2.057(2)$ |
| $g_\parallel = 2.240(3)$ | $g_\parallel = 2.243(4)$ |
| $2\alpha = 110.9°$ | $2\alpha = 109.9°$ |
| $\theta_m = 140.2°$ | $\theta_m = 141.5°$ |
| $\phi_m = 117.8°$ | $\phi_m = 112.7°$ |

[a] $(g^2)_1$, $(g^2)_2$ and $(g^2)_3$ and $\mathbf{a}_1$, $\mathbf{a}_2$ and $\mathbf{a}_3$ are the eigenvalues and eigenvectors of the $\boldsymbol{g}^2$ tensor in the $xyz = abc^*$ coordinate system. The values of $g_\perp$ and $g_\parallel$, the polar and azimuthal angles $\theta_m$ and $\phi_m$ of the normal to the square of ligands to copper ions and the angle $2\alpha$ between the normals to copper ions in sites A and B are also included.

$O_{eq}$–Cu–$O_{ax}$ interaction of adjacent Cu(L-threon)$_2$ molecules in a chain provides the main path for the transmission of the super-exchange coupling between copper unpaired electrons [16,18]. Neighboring chains in the crystal are coupled through complex chemical paths, including bonds of different type, which produce a 3D magnetic network of copper ions. These paths will be discussed below.

### 3.2. EPR data

#### 3.2.1. The g-factor

A single Lorentzian-shaped EPR line was observed in Cu(L-threon)$_2$·H$_2$O at 9.8 and 33.3 GHz for any magnetic-field orientation. Fig. 2 shows the angular variation of the experimental values for the squared $g$-factor ($g^2(\theta, \phi)$) obtained at 9.8 GHz. The experimental data of $g^2(\theta, \phi)$ at 33.3 GHz are similar to those at 9.8 GHz (data not shown). There are two copper ion sites with different spatial orientation, called sites A and B, in the crystal structure of the compound, related by a $C_2$ rotation around $b$. Thus, in the absence of exchange, we should expect two EPR resonance lines in the $ab$ and $cb$ planes. On the contrary, the copper ions are magnetically equivalent in the $ac$ plane, and, therefore their resonance lines cannot be distinguished. The fact that a single resonance line is observed in the three crystallographic planes, even at 33.3 GHz, indicates that the exchange interaction is large enough to collapse the hyperfine interaction with the copper nucleus ($I = 3/2$) and the nitrogen ligands ($I = 1$), and the resonance lines of the magnetically non-equivalent copper ions.

The angular variation of the position of the single exchange-collapsed resonance line observed at both microwave frequencies was evaluated assuming a Zeeman Hamiltonian of the type

$$H = \mu_B \mathbf{S}\boldsymbol{g}\mathbf{B} \quad (1)$$

where $\mu_B$ is the Bohr magneton, $\mathbf{S}$ is the effective spin operator ($S = 1/2$), $\boldsymbol{g}$ is the crystal $\boldsymbol{g}$-tensor defined as the average of the molecular $\boldsymbol{g}_i$ tensors ($i$ = A, B), and $\mathbf{B}$ is the applied magnetic field. The components of the crystal $\boldsymbol{g}$-tensor defined in Eq. (1) were obtained by fitting the function $g^2(\theta, \phi) = \mathbf{h}\boldsymbol{g}^2\mathbf{h}$ to the experimental data, where $\mathbf{h} = \mathbf{B}/|\mathbf{B}| = \sin\theta\cos\phi, \sin\theta\sin\phi, \cos\theta$ is the direction of the applied magnetic field $\mathbf{B}$ (see Fig. 2). The components of $\boldsymbol{g}^2$ at each microwave frequency, its eigenvalues and eigenvectors, are given in Table 3. They were used to obtain the solid lines in Fig. 2.

To evaluate the molecular $\boldsymbol{g}_i$-tensors of the copper ions in Cu(L-threon)$_2$·H$_2$O, we followed the procedure reported in Ref. [19] assuming axially symmetric molecular $\boldsymbol{g}$-tensors. We define $\theta_m$ and $\phi_m$ as the polar and azimuthal angles corresponding to the direction along which $g_\parallel$ is measured for copper ions in sites A, and $2\alpha$ as the angle between the normals to the sites A and B. We calculated $g_\perp$, $g_\parallel$, $\theta_m$ and $\phi_m$ using the values of the four non-zero components of the crystal $\boldsymbol{g}$-tensor (see Table 3). The values of the angles $\theta_m$ and $\phi_m$ are in a good agreement with the crystallographic results ($\theta_m = 139.3°$, $\phi_m = 119.5°$, and $2\alpha = 110.9°$) and support the assumption of axial symmetry for the copper site. The results obtained for the molecular $g$-factors indicate that the ground state orbital of the Cu ions is $d_{x^2-y^2}$ [20].

*3.2.2. The linewidth*

Several contributions to the EPR linewidth originated by interactions such as dipolar, hyperfine, and residual Zeeman have been identified in copper–amino acid complexes [21–25]. In most cases these different contributions to the angular variation of the linewidth have a strong cross-correlation, making difficult their identification and individual analysis. Exceptions are the frequency-dependent contribution arising from the existence of magnetically non-equivalent copper ions in the crystal lattice [4,26] and that observed in low-dimensional magnetic systems [21,27].

The linewidth data in Cu(L-threon)$_2$·H$_2$O at both microwave frequencies do not show significant differences in the *ab* and *c*a* planes (data not shown). On the other hand, a small but detectable frequency-dependent contribution was observed in the *c*b* plane (see Fig. 3(a)), the plane where the difference between the *g*-factors of the magnetically non-equivalent copper ions is largest. Although the crystal structure of Cu(L-threon)$_2$·H$_2$O is composed of copper chains along the crystallographic *b* axis, the angular variation of the linewidth data does not correspond to a 1D magnetic behavior. This fact suggests that the exchange parameters associated with the chemical paths connecting the copper ions of different chains are large enough to produce 3D spin dynamics, instead of that expected for a chain compound.

In order to evaluate the frequency-dependent contribution observed in the *c*b* plane, the experimental linewidth data were least squares fitted to a Fourier series to obtain the difference between the linewidths at 9.8 and 33.3 GHz (see Fig. 3(b)). This difference was least squares fitted with the function

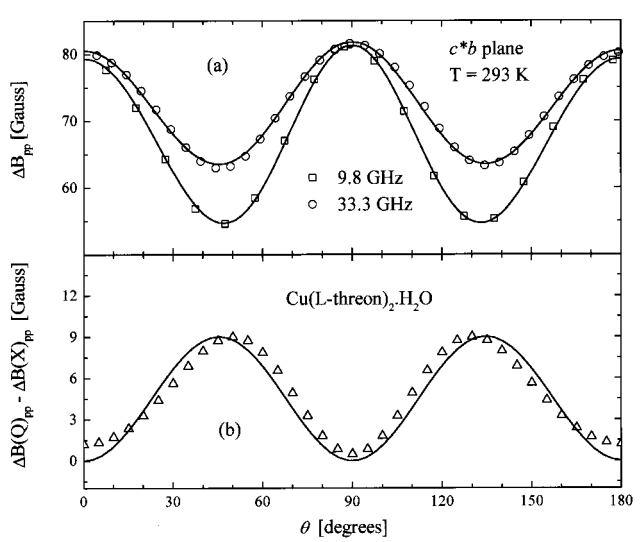


Fig. 3. (a) Angular variation of the EPR peak-to-peak linewidth at the Q- and X-bands. The solid lines correspond to a fitting of the data to Fourier series. (b) Linewidth difference. The solid line is a least-squares fit of the data with Eq. (2) in the text.

$$\Delta B_{pp}(Q) - \Delta B_{pp}(X) = \frac{\sqrt{\frac{2}{3}}\pi[\omega_o^2(Q) - \omega_o^2(X)]h}{8\pi g^3 \omega_e \mu_B}\,[g_A(\theta,\ \phi) - g_B(\theta,\ \phi)]^2 \qquad (2)$$

which takes into account the frequency-dependent contribution to the linewidth for a system with two magnetically non-equivalent copper ions per unit cell [26]. In Eq. (2), $\Delta B_{pp}(Q)$ and $\Delta B_{pp}(X)$ are the peak-to-peak linewidths at the Q- and X-bands, respectively, $\omega_o(Q) = 2\pi \times 33.3$ GHz and $\omega_o(X) = 2\pi \times 9.8$ GHz are the Larmor frequencies, $\omega_e$ is the exchange frequency, *h* is the Planck's constant, and *g* is the isotropic crystal *g*-factor in the *c*b* plane. As shown in Fig. 3(b), a good agreement was obtained between the values corresponding to the linewidth difference and the proposed function. The small discrepancies observed may be attributed to non-secular contributions to the linewidth which are relevant only at X-band [28,29]. From this fitting we obtained $\omega_e = 4.65 \times 10^{11}\ s^{-1}$ which, in turn, is associated with the exchange parameter through the relation [26]

$$\omega_e^2 = \frac{4\pi^2}{h}\ \sum_i Z_i\, J_i^2 \qquad (3)$$

where the $J_i$ values are the exchange parameters associated with the chemical paths linking magnetically non-equivalent copper ions pairs. $Z_i$ is the number of nearest copper neighbors connected by the *i*th chemical path. In Eq. (2), an exchange Hamiltonian of the form $H_{ex} = J\mathbf{S}_i\mathbf{S}_j$ was assumed.

*3.2.3. Super-exchange paths*

Fig. 4 shows three of the possible chemical paths for transmitting super-exchange interaction that involve only equatorial ligands of the copper ions. These paths connect pairs of magnetically non-equivalent copper ions at the distances of 9.07, 9.39 and 12.34 Å and are associated with the exchange constants $J_1$, $J_2$ and $J_3$, respectively. For clarity, only half of the molecules surrounding a copper ion at the general position *xyz* ($Cu_A$) have been included. As seen in this figure, the ions are connected through chemical paths having a variable number of diamagnetic atoms and bonds of different type, forming a complex 3D network. These paths involve a carboxylate bridge, the amino acid side chain, and one or two hydrogen bonds depending on the case. In two of them ($J_2$ and $J_3$), a non-coordinated water molecule is involved. This suggests a role of the hydrogen bonds provided by these lattice water molecules in the transmission of the super-exchange interaction between the metal centers.

There are also four remaining non-equivalent neighboring copper ions at 5.87 and 6.36 Å, respectively (not shown in Fig. 4), which are connected by chemical paths similar to the paths described above, and might

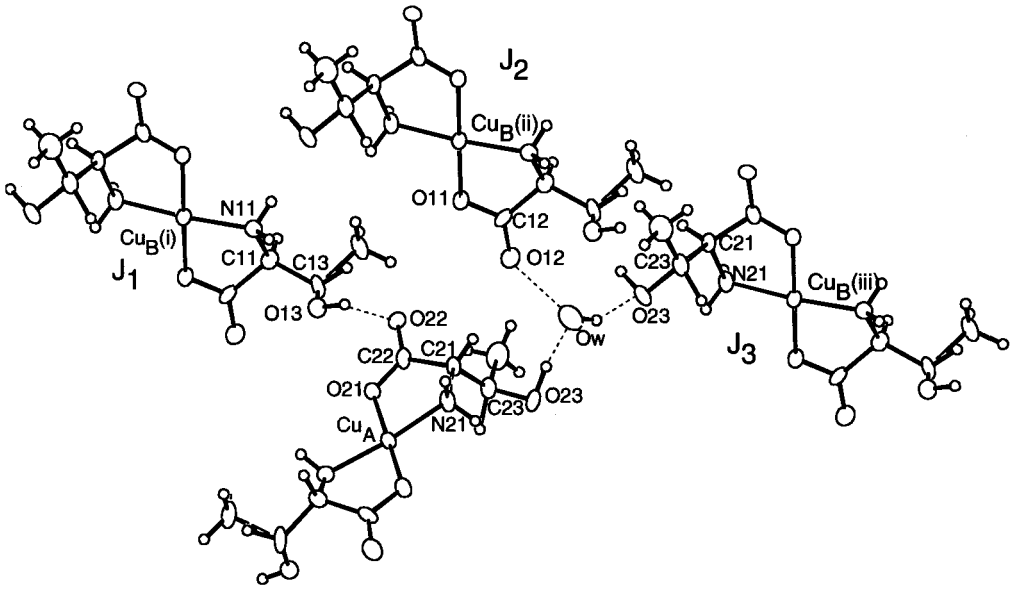


Fig. 4. Chemical paths mediating super-exchange interactions between the Cu(II) ion at the lower center complex and copper ions on neighboring, magnetically non-equivalent, complexes. These have been labeled after the coupling constants $J_1$–$J_3$ describing their interaction with the central complex. For simplicity, only half of the molecules surrounding this complex have been included in the plot. The other half is related to the one represented through translations along *b*. Dashed lines indicate H-bond interactions. Symmetry code: (i) $-1-x, 3/2+y, -z$; (ii) $-x, 3/2+y, -z$; (iii) $-x, 1/2+y, -1-z$.

also be considered as possible super-exchange paths. However, they involve an equatorial–apical interaction with one of the copper ions, and hence their strength can be neglected when compared to the other paths [2].

The absence of a low dimensional behavior in the linewidth data suggests that $J_1$, $J_2$, and $J_3$ have the same order of magnitude. Assuming $Z = 6$ nearest copper neighbors and $J_1 \cong J_2 \cong J_3$, a parameter $|J|/k =$ 1.45(5) K is estimated from Eq. (3). This result is in agreement with the value $|J|/k \geq 130$ mK obtained from the collapse condition $J \geq \Delta g \mu_B \mathbf{B}$ at the Q-band.

As shown in Fig. 1, Cu(L-threonine)$_2 \cdot H_2O$ has a chain structure with three diamagnetic atoms bridging neighboring, magnetically equivalent Cu(II) ions in a chain. Magneto structural correlations performed on copper amino acid complexes, having this carboxylate bridge topology as the main super-exchange path, suggest that the intra-chain exchange parameter in Cu(L-threon)$_2 \cdot H_2O$ should be smaller than 0.1 K [30]. This value represents less than 10% of the value obtained for $|J|/k$ in this work and explains why the angular variation of the linewidth data in this system does not correspond to that observed in a 1D system.

## 4. Conclusion

The present EPR data for Cu(L-threon)$_2 \cdot H_2O$ reported here indicate inter-chain super-exchange interaction with a magnitude of about 1.5 K between the closest, magnetically non-equivalent copper $d_{x^2-y^2}$ orbitals. To our knowledge, there are few studies dealing with compounds having long super-exchange chemical paths composed by H-bonds and saturated and non-saturated hydrocarbon chains. Balagopalakrishna and Rajasekharan [31] evaluated an exchange parameter $|J|/k \geq 0.084$ K (0.168 K for our notation for $H_{ex}$) for a chemical path similar to that found in Cu(L-threon)$_2 \cdot H_2O$, involving also two H-bonds but including 13 diamagnetic atoms. On the other hand, in previous studies performed on Cu(asp)phen, an exchange parameter $|J|/k = 1.44(2)$ K, similar to that observed in Cu(L-threon)$_2 \cdot H_2O$, was obtained, but for a chemical path formed by a carboxylate bridge and a hydrogen bond [6]. Compared with these previous results, we may conclude that the exchange parameter obtained in Cu(L-threon)$_2 \cdot H_2O$ is appreciably large for an electronic path achieving their connectivity through H-bonds and saturated and non-saturated sigma bonds. This fact would indicate a favorable orientation of both molecular σ-skeleton bridged by H-bonds within each super-exchange path (see Fig. 4). Intra-chain Cu–Cu coupling is, on one hand, enhanced by a shorter path but, on the other hand, reduced by longer apical O···Cu···O bonds and small overlap of Cu(II) $3d_{x^2-y^2}$ orbital with unfavorably oriented oxygen lone pair orbitals.

## 5. Supplementary material

X-ray crystallographic files are deposited in the Cambridge Crystallographic Data Centre under CCDC No. 140474. Copies of this information may be obtained free of charge from: The Director, CCDC, 12 Union Road, Cambridge, CB2 1EZ, UK (fax: +44-1223-336-033; e-mail: deposit@ccdc.cam.ac.uk or www: http://www.ccdc.cam.ac.uk).

## Acknowledgements

This work was supported by the Universidad Nacional del Litoral (CAI + D 291) and the Consejo Nacional de Investigaciones Científicas y Técnicas (CONICET) of Argentina, the Conselho Nacional de Pesquisas (CNPq), the Fundação de Amparo a Pesquisa do Estado de São Paulo (FAPESP), the Financiadora de Estudos e Projetos (FINEP), and the Antorchas and Vitae Foundations of Brazil. Some of the X-ray measurements were carried out at the National Diffraction Laboratory (LANADI), La Plata, Argentina. A.C.R. and C.D.B. would like to thank Professor R. Calvo for the fruitful discussions and for introducing them to the field.

## References

[1] R.D. Willet, D. Gatteschi, O. Kahn (Eds.), Magneto–Structural Correlations in Exchange Coupled Systems, NATO ASI Series C, vol. 140, Reidel, Dordrecht, 1984.
[2] O. Kahn, Molecular Magnetism, VCH, New York, 1993.
[3] M.J. Romão, J. Knäblein, R. Huber, J.J.G. Moura, Prog. Biophys. Molec. Biol. 68 (1997) 121.
[4] C.D. Brondino, N.M.C. Casado, M.C.G. Passeggi, R. Calvo, Inorg. Chem. 32 (1993) 2078.
[5] D.M. Martino, M.C.G. Passeggi, R. Calvo, O.R. Nascimento, Physica B 225 (1996) 63.
[6] C.D. Brondino, R. Calvo, A.M. Atria, E. Spodine, O.R. Nascimento, O. Peña, Inorg. Chem. 36 (1997) 3183.
[7] C.D. Brondino, R. Calvo, A.M. Atria, E. Spodine, O. Peña, Inorg. Chim. Acta 228 (1995) 261.
[8] A. Bencini, D. Gatteschi, Electron Paramagnetic Resonance of Exchange Coupled Systems, Springer, Berlin, 1989.
[9] S.K. Hoffmann, W. Hilczer, J. Goslar, Appl. Magn. Reson. 7 (1994) 289 and Refs. cited therein.
[10] V. Amirthalingam, K.V. Muralidharan, Pramana 4 (1975) 83.
[11] G.M. Sheldrick, SHELX, Program for Crystal Structure Determination, University of Cambridge, Cambridge, 1976.
[12] B.A. Frenz, Enraf–Nonius Structure Determination Package, Enraf–Nonius, Delft, The Netherlands, 1983.
[13] W.R. Busing, H.A. Levy, Acta Crystallogr. 10 (1957) 180.
[14] C.K. Johnson, ORTEP, Report ORNL-3794, Oak Ridge, TN, 1965.
[15] W.C. Hamilton, Acta Crystallogr. 12 (1959) 609.
[16] P.R. Levstein, R. Calvo, E.E. Castellano, O.E. Piro, B.E. Rivero, Inorg. Chem 29 (1990) 3918.
[17] T.G. Fawcett, M. Ushay, J.P. Rose, R.A. Lalancette, J.A. Potenza, H.J. Schugar, Inorg. Chem. 18 (1979) 327.
[18] M.L. Siqueira, R.E. Rapp, R. Calvo, Phys. Rev. B 48 (1993) 3257.
[19] R. Calvo, M.A. Mesa, Phys. Rev. B 28 (1983) 1244.
[20] H.J. Zeiger, G.W. Pratt, Magnetic Interactions in Solids, Oxford University Press, London, 1973.
[21] A.M. Gennaro, P.R. Levstein, C.A. Steren, R. Calvo, Chem. Phys. 111 (1987) 431.
[22] H. Yokoi, S. Ohsawa, Bull. Chem. Soc. Jpn. 46 (1973) 2766.
[23] P.R. Newman, J.M. Imes, J.A. Cowen, Phys. Rev. B 13 (1976) 4093.
[24] (a) R. Calvo, M.A. Mesa, G. Oliva, J. Zukerman-Schpector, O.R. Nascimento, M. Tovar, R. Arce, J. Chem. Phys. 81 (1984) 4584. (b) R. Calvo, M.A. Mesa, Phys. Lett. A 108 (1985) 217.
[25] R. Calvo, H. Isern, M.A. Mesa, Chem. Phys. 100 (1985) 89.
[26] P.R. Levstein, C.A. Steren, A.M. Gennaro, R. Calvo, Chem. Phys. 120 (1988) 449.
[27] (a) P.M. Richards, M.B. Salamon, Phys. Rev. B 9 (1974) 32. (b) P.M. Richards, in: K.D. Mueller, A. Rigamonti (Eds.), Local Properties at Phase Transitions, North Holland, Amsterdam, 1976.
[28] A.M. Gennaro, R. Calvo, J. Phys. Condens. Matter 1 (1989) 7061.
[29] R. Calvo, M.C.G. Passeggi, M.A. Novak, O.G. Symko, S.B. Oseroff, O.R. Nascimento, M.C. Terrile, Phys. Rev. B 43 (1991) 1074.
[30] P.R. Levstein, R. Calvo, Inorg. Chem 29 (1990) 1581.
[31] C. Balagopalakrishna, M.V. Rajasekharan, Phys. Rev. B 42 (1990) 7794.